

Jennifer Mueller*, Hartwig Deneke, Victor Venema, Clemens Simmer
Meteorological Institute of the University Bonn, Bonn, Germany

1. Introduction

Clouds play an important part in the energy budget of the earth. They reflect solar radiation and thus cool the earth, but also emit longwave radiation to the surface and hence contribute to the natural greenhouse effect. It is difficult to quantify the influence of clouds on the budget because of a lack of accurate global observations of cloud microphysical properties and radiation fluxes. A new possibility of observing clouds and aerosols is provided by the satellites CloudSat (Stephens et al., 2002) and CALIPSO (Winker et al., 2009). Both carry active instruments (the Cloud Profiling Radar CPR and the Cloud and Aerosol Lidar with Orthogonal Polarization CALIOP) and are therefore able to resolve the vertical structure of clouds and aerosol layers. Another fundamental problem is that radiative transfer in climate models needs to be calculated with strong simplifications in the radiative transfer parameterizations. Important simplifications typically made are to solve the radiative transfer problem in 1D instead of 3D and describe the influence of non-resolved cloud structure by a small number of parameters. In this study, the new active satellite data together with the Rapid Radiative Transfer Model for Global climate models (RRTMG) (Iacono et al., 2008) are used to estimate the influences of sub-scale cloud variability and parameterization uncertainties in radiation schemes.

2. Methods

Data from CloudSat and CALIPSO are used to run RRTMG. This model is based on a 2-stream solver for the radiative transfer equation and a correlated-k scheme for absorption by relevant atmospheric gases. The radiative fluxes are then compared to the radiative flux product 2B-FLXHR described by L'Ecuyer et al. (2008). The comparisons are performed for 200 orbits from 1st July 2008 until 15th July 2008. All plots shown below display results for orbit number 11772. This orbit started on 14th July 2008 at 17:21 UTC and was chosen because it has a particular large land fraction of 55% (50% of daylight columns). Additionally mean values and corre-

lations between RRTMG results and 2B-FLXHR for all orbits of the period have been calculated.

The main input for RRTMG is cloud data which is taken from the 2B-CWC-RO product retrieved by a modification of the algorithm described in (Austin and Stephens, 2001) using mainly the 2B-GEOPROF product as input (CIRA, 2007). Furthermore, atmospheric state variables from reanalysis data of the ECMWF-AUX product as well as surface albedo data and surface emissivity data based on 20 scene types from maps provided by the NASA CERES/SARB working group (NASA, 2010) are used as input for RRTMG. Aerosol data are taken from CALIPSO inferred aerosol extinction at 532 nm. Those data are converted to broadband aerosol properties with the help of the Optical Properties of Aerosols and Clouds (OPAC) library (Hess et al., 1998).

At first only clear sky fluxes will be compared. These fluxes do not include aerosol effects, because the 2B-FLXHR product is calculated without aerosols. In the second part the impact of aerosols is taken into account, and finally clouds are included into the calculations with RRTMG.

3. Clear Sky

To separate differences that occur because of different treatments of the atmosphere from those that arise from different treatment of clouds, at first only clear sky fluxes are compared. These are automatically calculated by both radiative schemes by ignoring the cloud input. Figures 1 and 2 show the shortwave (sw) respectively longwave (lw) fluxes of RRTMG (black line) along orbit 11772 together with the difference to 2B-FLXHR (red line). It can be seen that the incoming solar radiation at the top of the atmosphere (TOA) is somewhat higher in 2B-FLXHR. The mean difference for the daylight columns of all orbits is 2.3 Wm^{-2} (see Table 1), indicative of differences in the solar constant used in both schemes.

The differences at the surface (SFC) are noticeable higher and of opposite sign with 13.2 Wm^{-2} . Previous investigations (Arking, 1996) showed that radiative transfer models at that time tended to underestimate absorption by the atmosphere. This finding suggests that - despite substantial efforts

* Corresponding author address: Jennifer Müller, University Bonn, Meteorological Institute, Auf dem Hügel 20, 53121 Bonn, Germany; e-mail: jenny.mueller.86@googlemail.com

	Corr.	RRTMG	2B-FLXHR
sw down TOA	1.00	882.1	884.4
sw down SFC	1.00	677.0	690.9
sw up SFC	0.84	88.7	66.9
sw up TOA	0.84	124.0	110.7
lw up SFC	0.99	406.7	409.0
lw up TOA	0.99	269.7	268.0
lw down SFC	0.99	318.9	328.8

TAB. 1: Correlations of clear sky fluxes between RRTMG and 2B-FLXHR and mean values of the respective fluxes.

in the mean time - models still disagree about the shortwave absorption by atmospheric gases.

Another difference between RRTMG and 2B-FLXHR is shown in the lower panels of Figure 1. The assumptions according the surface albedo differ. Our input to RRTMG is based on 20 IGBP scene type maps from the NASA CERES/SARB working group, whereas the albedo of 2B-FLXHR is based on seasonally varying data. We have calculated mean broad band albedos grouped by scene type as ratio of upwelling and downwelling shortwave radiation at the surface. The albedo values of 2B-FLXHR vary within the scene types as well. An extract of the results are shown in Table 2. The albedos for some scene types are in good agreement (e.g. tundra), but some differ significantly like crops or ice.

The longwave fluxes displayed in Figure 2 show better correspondence. Especially the longwave radiation emitted by the earth is well reproduced. Some differences occur because 2B-FLXHR assumes a black surface in the infrared regime, while RRTMG employs scene type-dependent emissivities. By comparing upwelling fluxes at TOA to downwelling fluxes at the surface (better to be seen in Table 1 than in Figure 2) it can be found that the atmosphere in RRTMG is optically thinner for the longwave range compared to 2B-FLXHR, while it is thicker for shortwave radiation.

Scene type	RRTMG	2B-FLXHR	SD
Mixed Forest	0.16	0.09	0.05
Grassland	0.24	0.16	0.07
Crops	0.24	0.12	0.04
Snow/Ice	0.62	0.45	0.15
Barren/Desert	0.32	0.38	0.11
Water	0.07	0.05	0.01
Tundra	0.17	0.16	0.12

TAB. 2: Broadband albedo calculated by dividing the upwelling shortwave radiation at the surface by the downwelling as well as standard deviation (SD) of 2B-FLXHR for some scene types defined by IGBP.

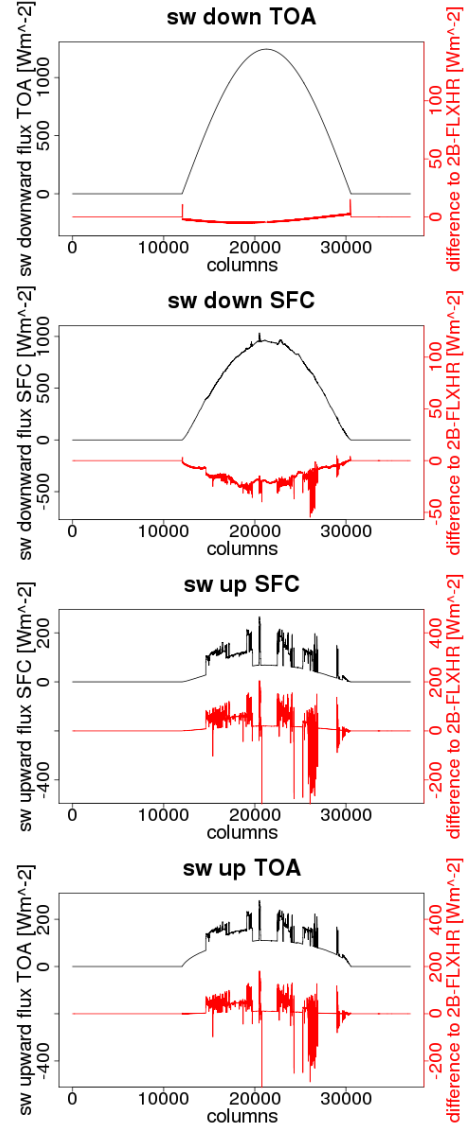


FIG. 1: Shortwave clear sky fluxes of RRTMG (black line) and the difference to 2B-FLXHR (red line) for orbit 11772. The right axis belongs to the red differences.

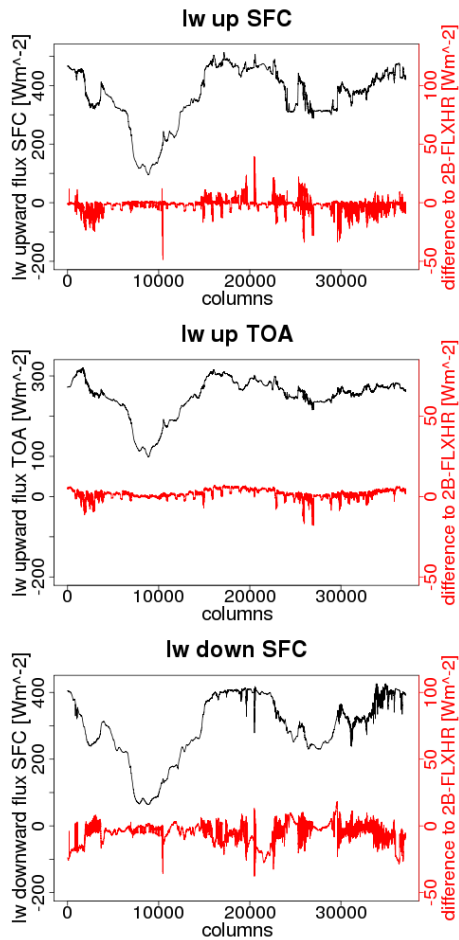


FIG. 2: Longwave clear sky fluxes of RRTMG (black line) and the difference to 2B-FLXHR (red line) for orbit 11772. The right axis belongs to the red differences.

4. Aerosols

The current version of the CloudSat 2B-FLXHR product neglects aerosol effects. Using the recently released CALIPSO 5 km V3.01 aerosol profile product, we have analyzed 49 CALIPSO daytime orbits from 22nd to 25th July 2008 for a rough estimate of the direct aerosol effect on the clear sky shortwave radiation budget. To obtain broadband aerosol properties, the CALIPSO aerosol types have been mapped to OPAC types (Hess et al., 1998).

As an example, the influence of aerosols on shortwave downwelling radiation at the surface is shown in Figure 3 and on upwelling shortwave radiation at TOA in Figure 4 for a thick aerosol layer. Additionally, averaged values of transmittance and reflectance have been calculated for clear sky columns of all 49 orbits. The results show that the downwelling shortwave irradiance

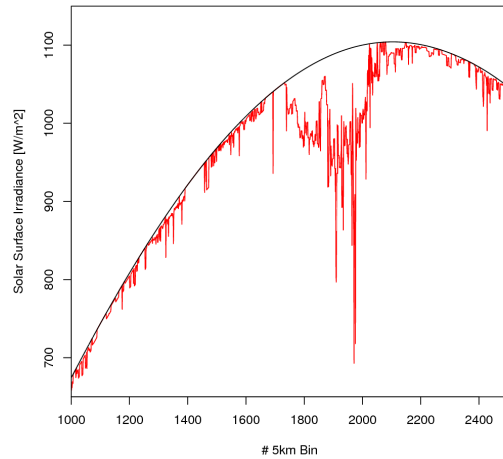


FIG. 3: Influence of an aerosol layer on the downwelling clear sky shortwave radiation at SFC.

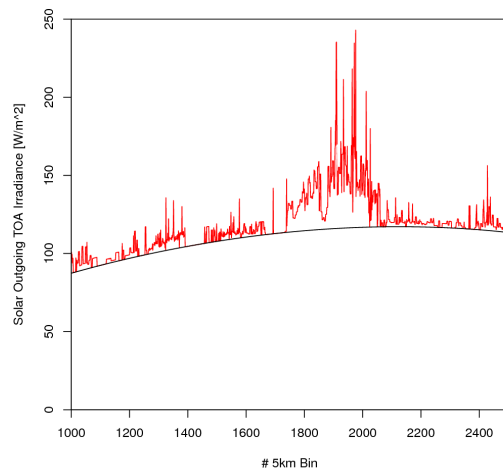


FIG. 4: Influence of an aerosol layer on the upwelling clear sky shortwave radiation at TOA.

	Corr.	RRTMG	2B-FLXHR
sw down SFC	1.00	258.9	267.8
sw up TOA	1.00	498.3	504.36
lw up TOA	0.95	264.5	257.9
lw down SFC	0.98	422.6	422.7

TAB. 3: Correlations of fluxes of columns with pure water clouds between RRTMG and 2B-FLXHR and mean values of the respected fluxes.

is reduced by 21.2 Wm^{-2} (2.3% of clear-sky irradiance), while reflected atmospheric irradiance at TOA is increased by 5.5 Wm^{-2} (0.8%). Absorption of solar radiation within the atmosphere is increased through aerosol from 83.1 Wm^{-2} (9.4%) to 95.9 Wm^{-2} (10.6%).

5. Clouds

The results for the cloudy sky are not as clear as those for clear sky and aerosols. In case of pure water clouds, the calculated fluxes are in reasonable agreement between RRTMG and 2B-FLXHR. This is shown in Table 3. The mean incoming sw radiation at the SFC is decreased to 36% of the clear-sky flux of the same columns in both models. Model differences are smaller than those found for the clear sky calculations of the same columns (not shown).

The correlation for longwave fluxes are lower than those for the shortwave fluxes or the for clear sky cases. While RRTMG increases the longwave downwelling radiation by 17% compared to the clear sky fluxes, 2B-FLXHR adds 15%. The longwave upward radiation at TOA is decreased to 95% of the clear-sky radiation by RRTMG respectively to 98% by 2B-FLXHR. In summary water clouds are optically thicker for longwave radiation in RRTMG.

In contrast to the results for pure water clouds, the correlations for ice and mixed phase clouds are quite low. We expect that the deviations are caused by different assumptions about cloud optical properties. Furthermore, large differences were found for cloud columns containing some missing data points. Care has thus to be taken in interpreting these columns.

6. Conclusion

In many aspects, our results show encouraging agreements with the 2B-FLXHR product. Nevertheless, the observed differences demonstrate the significant uncertainties which are introduced into model-based estimates of the radiation budget, re-

lated to choices in the treatment of surface albedo, gaseous absorption, and cloud properties.

REFERENCES

- Arking, A., 1996, Absorption of solar energy in the atmosphere: Discrepancy between model and observations, *Science*, 273, 779–782.
- Austin, R. and G. L. Stephens, 2001, Retrieval of stratus cloud microphysical parameters using millimeter-wave radar and visible optical depth in preparation for cloudsat, 1. algorithm formulation.
- CIRA, 2007, Level 2B radar-only Cloud Water Content (2B-CWC-RO) process description document, http://www.cloudsat.cira.colostate.edu/ICD/2B-CWC-RO/2B-CWC-RO_PD_5.1.pdf.
- Hess, M., P. Koepke, and I. Schult, 1998, Optical properties of aerosols and clouds: the software package OPAC, *Bul. Am. Met. Soc.*, 79, 831–844.
- Iacono, M., J. S. Delamere, E. J. Mlawer, M. W. Shephard, S. A. Clough, and W. D. Collins, 2008, Radiative forcing by long-lived greenhouse gases: Calculations with the AER radiative transfer models, *J. Geophys. Res.*, doi:10.1029/2008JD009944.
- L'Ecuyer, T. S., N. B. Wood, T. Haladay, G. L. Stephens, and P. W. Stackhouse Jr., 2008, Impact of clouds on atmospheric heating based on the r04 cloudsat fluxes and heating rates data set, *J. Geophys. Res.*, doi:10.1029/2008JD009951.
- NASA, Surface and Atmospheric Radiation Working Group, 2010, NASA Langley Research Center, <http://www-surf.larc.nasa.gov/surf/index.html>.
- Stephens, G. L., D. G. Vane, R. J. Boain, G. G. Mace, K. Sassen, Z. Wang, A. J. Illingworth, E. J. O'Connor, W. B. Rossow, S. L. Durden, S. D. Miller, R. T. Austin, A. Benedetti, C. Mitrescu, and CloudSat Science Team, 2002, The CloudSat mission and the A-TRAIN: A new dimension to space-based observations of clouds and precipitation, *Bull. Am. Met. Soc.*, doi:10.1175/BAMS-83-12-1771.
- Winker, D. M., M. A. Vaughan, A. Omar, Y. Hu, K. A. Powell, Z. Liu, W. H. Hunt, and S. A. Young, 2009, Overview of the CALIPSO mission and CALIOP data processing algorithms, *J. Atm. Ocean. Tech.*, doi:10.1175/2009JTECHA1281.1.